GFZ
Helmholtz-Zentrum
POTSDAM

Originally published as:

Diez Zaldívar, E. R., Priolo, E., Grigoli, F., Cesca, S. (2016): Misalignment Angle Correction of Borehole Seismic Sensors: The Case Study of the Collalto Seismic Network. - *Seismological Research Letters*, *87*, 3, pp. 668—677.

DOI: http://doi.org/10.1785/0220150183

Seismological Research Letters

This copy is for distribution only by
the authors of the article and their institutions
in accordance with the Open Access Policy of the
Seismological Society of America.

For more information see the publications section
of the SSA website at www.seismosoc.org

THE SEISMOLOGICAL SOCIETY OF AMERICA
400 Evelyn Ave., Suite 201
Albany, CA 94706-1375
(510) 525-5474; FAX (510) 525-7204
www.seismosoc.org

Misalignment Angle Correction of Borehole Seismic Sensors: The Case Study of the Collalto Seismic Network

by Eduardo R. Diez Zaldívar, Enrico Priolo, Francesco Grigoli, and Simone Cesca

ABSTRACT

One of the most critical problems affecting seismological data acquisition is related to possible misorientation of three-component seismic sensors. This generally happens when their orientation cannot be measured directly, as in the case of sensors deployed in boreholes. We describe here the sensor reorientation procedure of the Collalto Seismic Network, a microseismic monitoring network located in northeastern Italy that consists of 10 broadband three-component stations deployed in boreholes. We apply a procedure based on the misfit minimization of a complex trace recorded by a given station with respect to a reference station for which orientation is known. The main advantage of this methodology is that the reorientation of seismic sensors can be viewed as a linear inverse problem in the complex domain, which ensures that the preferred solution corresponds to the global minimum of a misfit function. Furthermore, it is also possible to simultaneously use more than one seismic event to better constrain the solution of the inverse problem. In this article, we further compare the orientation results obtained for a seismometer–seismometer sensor pair with those obtained using an accelerometer–seismometer sensor pair. We finally show the reorientation results for all the stations of the network, obtained using eight teleseismic events that occurred between January 2012 and May 2014.

Online Material: Tables of station information and figure showing alignment results.

INTRODUCTION

One of the most critical problems affecting geophysical data acquisition, with particular focus to seismological applications, is related to the possible misorientation of three-component seismic sensors with respect to a common reference coordinate system, generally the geographic north. Misorientations may induce significant errors in several data analysis procedures (e.g., moment tensor inversion, polarization analysis, etc.), leading to incorrect results and interpretations. These problems usually occur when the orientation cannot be measured directly, as in the case of sensors deployed within boreholes or at the ocean bottom or when dealing with compass-oriented sensors deployed in areas with strong magnetic anomalies (e.g., volcanic or polar regions). For instance, three-component geophones in boreholes (Di Siena *et al.*, 1984) or free-fall ocean-bottom seismometers (OBSs) (Grigoli *et al.*, 2012) are generally deployed in an unknown random orientation.

Misorientation may concern all components. The correct alignment of the vertical component to the gravity field gradient is surely mostly important and critical from an instrumentation point of view; for instance, in modern force-balance seismometers, it may result in a reduction of the dynamic range and a higher electric consumption. The correction of the orientation to the vertical is done by acting physically on the sensor, the so-called horizontal leveling: when the sensor cannot be handled manually, this may be done either by directly exploiting the gravity force (a technique often used for OBSs landed on the seafloor at the end of a free fall) or by electric engines. However, most of the methods used for the reorientation of misaligned sensor are based on the approximation that the vertical axis orientation is sufficiently close to the correct one, so that any deviation from this can be neglected (Krieger and Grigoli, 2015).

Although less critical for the instrument than the vertical alignment, the alignment of the horizontal components to the adopted reference system (usually geographic north) is indeed very important for several analysis procedures, such as polarization analysis or moment tensor inversion. This problem is probably more difficult to solve when dealing with sensors that cannot be handled directly or when, with compass-based orientations, the Earth's magnetic field is altered (e.g., in volcanic and polar regions) or perturbed by external factors (e.g., the metallic casing of boreholes, installations in armed concrete vaults, etc.). Estimating and verifying the absolute orientation of the horizontal components is therefore a very important

 doi: 10.1785/0220150183

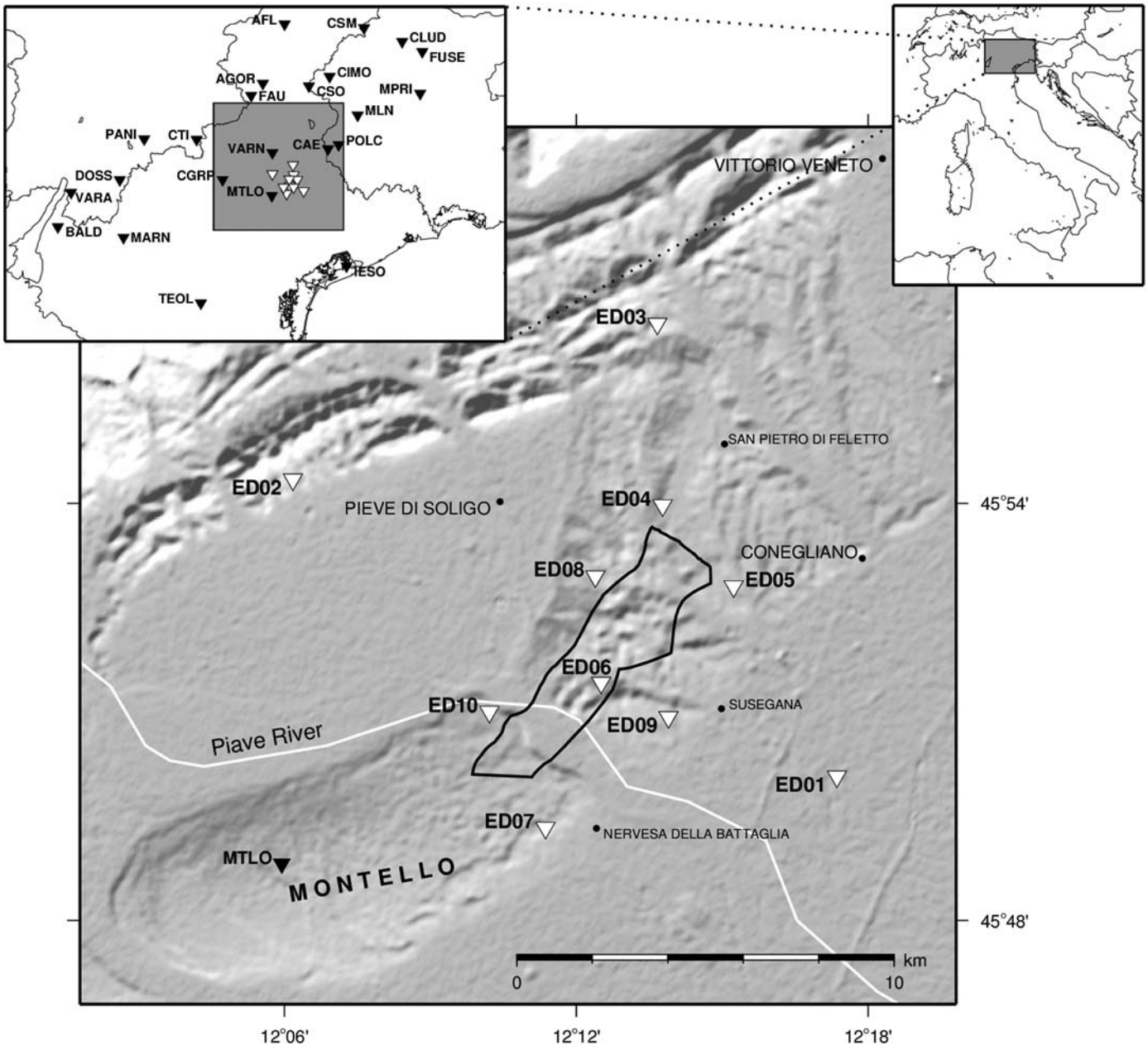

▲ **Figure 1.** Collalto Seismic Network location map. The gray shading represents topography. The black line represents the boundary of the underground storage area. The Collalto Seismic Network (RSC) stations are represented by inverted white triangles. The inverted black triangle represents the MTLO station, which belongs to the regional seismic network managed by the National Institute of Oceanography and Experimental Geophysics. The two insets provide the geographical framework of the study area; the inset to the left also shows the locations of the regional stations that enter into the RSC system. More details can be found in Priolo, Romanelli, *et al.* (2015).

step in establishing the quality of a single station or a seismic network.

The current techniques are based on seismic-signal polarization analysis or waveform cross correlation. For instance, Di Siena *et al.* (1984) proposed a power maximization of the first arrival of the *P* wave to determine the azimuthal orientation of three-component geophones deployed in boreholes. Different polarization-analysis-based orientation methods have been proposed by Becquey and Dubesset (1990), Michaels (2001), and Oye and Ellsworth (2005). On the other hand, Zheng and McMechan (2006) used cross correlation of traces to infer the relative orientation angles between adjacent geophone pairs in borehole arrays.

The orientation methods used for OBSs are quite similar to those used for borehole sensors. For instance, Nakamura *et al.* (1987) used air gun shots and the wave amplitude ratio of the two horizontal components to determine the location and orientation of OBSs. Hensch (2009) used the waveform

cross correlation to estimate the angle of alignment among OBSs in the Aegean Sea and inland stations, whereas Zha and Menke (2013) developed a method for determining the horizontal orientation of OBSs by analyzing the polarization of Rayleigh waves retrieved from ambient-noise cross correlation.

In this article, we describe the results obtained in estimating the horizontal orientation of the borehole sensors of the Collalto Seismic Network (in Italian, Rete Sismica di Collalto [RSC]), a local seismic network devoted to monitor-induced seismicity associated with natural gas storage operations in an underground depleted gas reservoir located in northeast Italy. We use the method developed by Grigoli *et al.* (2012), which estimates the relative orientation angles among different pairs of stations by fitting the complex traces of each station pair using a complex linear least-squares approach.

THE COLLALTO SEISMIC NETWORK

The Collalto gas storage concession, held by Edison Stoccaggio S.p.A., is located at the front of the southeastern Alps and at the northern margin of the Venetian Plain. The region is characterized by medium–high seismic hazard (Gruppo di Lavoro MPS, 2004). Thus, seismic monitoring is a key tool—not only to identify the microseismicity induced by gas storage operations, but also to understand whether and how this activity may interact with the tectonic structures surrounding the reservoir.

The reservoir is a geologic trap, with porous and permeable rock layers a few meters thick, sealed by impermeable formations, and located at 1500–1600 m depth (Picotti, 2007). It extends approximately over a 10 km × 4 km area (Fig. 1). Full details about the overall framework in which the RSC operates, as well as its technical features, are described in Priolo, Romanelli, *et al.* (2015), whereas a synthesis of the most important pieces of information for what concerns this study is reported hereafter.

The RSC is made up of 10 high-quality stations distributed in such a way as to cover the storage area more densely but at the same time to ensure adequate sensitivity for about 10–15 km around the storage. The goal is to reach completeness magnitude between 0 and 1 in a restricted area surrounding the reservoir, preserving the capability of recording nonsaturated signals for natural medium–strong events ($M_w \geq 5$) that might occur throughout the study area.

Of the total 10 stations, 9 are equipped with borehole Güralp CMG-SP1 sensors with 10 s natural period, whereas 1 (the ED06, which is also the central one in the network geometry) has a classical Güralp CMG-3T broadband sensor with 120 s natural period. For all stations, seismometers have been deployed at depths to reduce the impact of the natural or anthropic noise and thus improve the network detection threshold.

The depth of the sensors varies approximately from 13 to 33 m, with the exceptions of site ED01, which is located on the plain at a depth of 155 m, and site ED06, which hosts the broadband sensor at about 5 m depth. In addition, five sites are also equipped with force-balance accelerometers (Güralp CMG-5TC) deployed at the surface to ensure full dynamic range and proper estimation of the ground motion in the case of strong events.

All channels are digitized through a 24-bit Güralp CMG-DM24S3 or DM24S6 digitizer, depending on the number of acquisition channels.

The depth of the borehole sensors varies from about 13 to 155 m among the stations; depths are indicated in Ⓔ Table S1, available in the electronic supplement to this article, for each station. Site ED06 differs from all the other sites in its monumentation, which consists of a quite large housing, buried in the ground, that hosts the two sensors at the base at about 5 m depth. Here, sensors can be handled (and oriented) manually. Therefore, ED06 represents the reference station for estimating the orientation of all the others in our study.

To better evaluate the results we will present in this article, we need to describe how borehole sensors have been deployed. For the deepest site, ED01, where the borehole reaches 155 m depth, the sensor is lowered into the hole using a winch with no control on the horizontal orientation, which therefore remains unknown. In this case, the clamping mechanism, provided by Güralp, consists of a mechanical system that can be locked and unlocked from the surface by two iron wires (Fig. 2a–c). For the other eight stations, with borehole depth ranges between about 13 and 33 m, the sensor is equipped with a handmade mechanical equipment. It consists of an iron foil, placed externally to the sensor along its length, which flexes elastically as the sensor is inserted into the hole. By tuning its width, we obtain the optimal friction that keeps the sensor well clamped to the borehole walls but at the same time allows us to push or pull the sensor along the borehole when necessary (Fig. 2d). The sensor is pushed at the borehole bottom using a rigid polyvinyl chloride (PVC) pipe, which ends with a bayonet joint directly on the sensor. An iron wire, which runs within the pipe, is also fastened to the sensor. In this way, the sensor can be both pushed down or pulled up and rotated laterally in one sense. The rotation in the opposite side has the effect of unblocking the pipe from the sensor. More pipe segments can be added as the sensor depth increases. The sensor orientation is then controlled at the surface by rotating the PVC pipe directly so as to align a pre-signed mark to the north.

The deployment and orientation procedure described above has been applied consistently to all borehole sensors except for a few cases in which the sensor was deployed and removed repeatedly because of malfunctioning. This was the case with station ED09 during year 2013, for which the orientation was not carried out. Although we expect misalignment values in the order of some degrees (and in all cases within 5°–10°), we obviously expect a possible, relevant misalignment for ED09 borehole sensor.

METHOD

As already mentioned, we apply the method developed by Grigoli *et al.* (2012) to estimate the horizontal orientation of the RSC borehole seismometers with respect to a reference station for which the orientation can be measured and therefore is

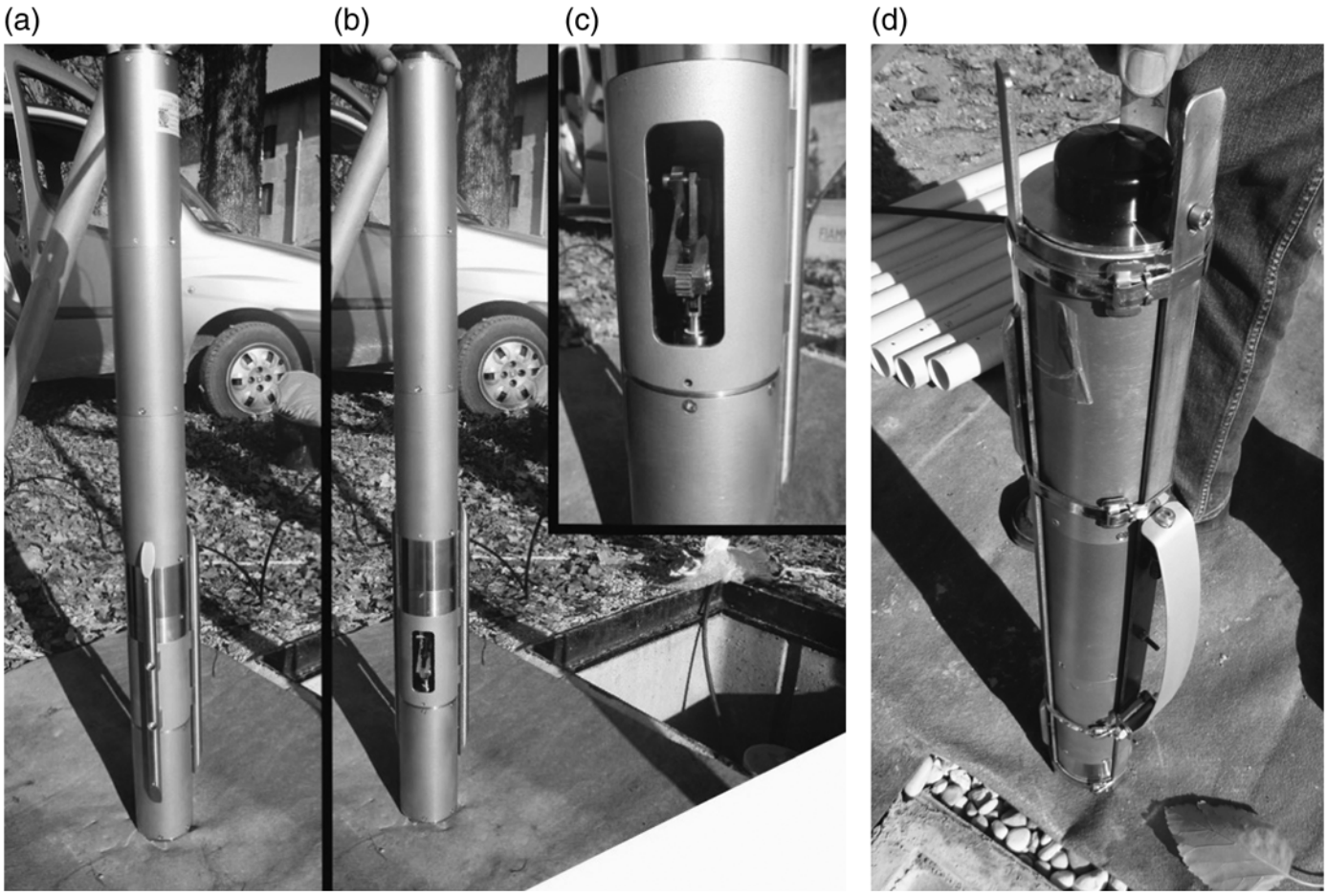

▲ **Figure 2.** Details about the clamping mechanism adopted for the RSC borehole stations. (a–c) Station ED01, where the sensor is deployed at 155 m depth. The clamping mechanism is that provided by Güralp, and it can be locked and unlocked remotely from the surface. (d) Handmade mechanical equipment used for the other stations where the sensor is deployed at less than 50 m depth. It consists of an iron foil, placed externally to the sensor along its length, which flexes elastically as the sensor is inserted into the hole. More details are provided in the text.

known. This method estimates the relative orientation of a sensor with respect to one or more reference sensors by minimizing the misfit between the recorded waveforms at each pair of stations. As for all the other methods based on the use of a reference station, this approach requires two main conditions: (1) plane-wave approximation of the recorded wavefield and (2) similarity of the measured signals between the reference station and the misoriented one. These conditions are generally satisfied for stations close enough to each other with respect to the dominant wavelength λ of the wavefield (i.e., $d \ll \lambda$, in which d is the interstation distance) and if no crust or ground heterogeneities are present at local scale among the used stations. To ensure that these conditions are satisfied, it is therefore convenient to analyze low-pass filtered waveforms related to far earthquakes or teleseismic events with clear S wave and surface wavetrains.

Under those assumptions, the misfit between waveforms recorded by the horizontal components of a couple or more sensors decreases as they become properly oriented (i.e., aligned) and, vice versa, increases with misalignment. The method provides the sign of the correction angle as well, that is, the sensor should be rotated clockwise or counterclockwise for negative or positive angle mismatch, respectively. The most effective way to determine the absolute orientation of a sensor is that to rotate the sensor relative to a reference sensor for which the absolute orientation is known.

In mathematical terms, the problem for the latter case is stated as follows (Grigoli *et al.*, 2012). Let us suppose we have n three-component stations for which the orientations are unknown. In most cases, the vertical component of a seismic sensor can be considered well oriented and only horizontal components need to be retrieved (Krieger and Grigoli, 2015). For this reason, our aim is to align the horizontal components of a generic kth station with respect to a reference one (denoted with R). We start by defining the complex seismic trace of the kth station $S_k(t)$ as

$$S_k(t) := X_k(t) + iY_k(t) = |X_k(t) + iY_k(t)| \exp[i\theta_k(t)], \quad (1)$$

in which i is the imaginary unit and $X_k(t)$ and $Y_k(t)$ are the horizontal-component records. We can write complex traces in a

more compact way using vector notation (in bold) and omitting the time variable t. The residuals vector $\mathbf{r}$ between the complex trace of the reference sensor $\mathbf{S}^R$ and the kth sensor $\mathbf{S}^k$ can be written as

$$\mathbf{r} = \mathbf{S}^R - \mathbf{S}^k \exp(-i\phi_k), \tag{2}$$

in which ϕ_k is the rotation angle of the kth sensor with respect to the reference sensor R. For the correct alignment angle, that is, $\phi_k = \theta_k - \theta_R$, we have

$$\phi_k \cong \min(||\mathbf{S}^R - \mathbf{S}^k \exp(-i\phi_k)||_2) := \min(||\mathbf{d} - \mathbf{G}\mathbf{m}||_2). \tag{3}$$

In analogy with the common notation used in inverse problem theory, $\mathbf{S}^R$ corresponds with the data vector $\mathbf{d}$, $\mathbf{S}^k$ corresponds with $\mathbf{G}$, and $\exp(-i\phi_k)$ is the model vector $\mathbf{m}$. Thus, in the complex domain, vector rotation can be performed by multiplying the vector itself with a complex exponential for which the phase is the rotation angle, and this angle can be found as a solution of the overdetermined linear inverse problem:

$$\mathbf{d} = \mathbf{G}\,\mathbf{m}. \tag{4}$$

The least-squares solution of this linear system of equations can be estimated by computing the generalized inverse in the complex domain, that is,

$$\mathbf{m} = (\mathbf{G}^{\mathrm{H}}\mathbf{G})^{-1}\mathbf{G}^{\mathrm{H}}\mathbf{d}, \tag{5}$$

in which H denotes the conjugate transpose matrix

$$m_k = \exp(i\phi_k) \tag{6}$$

and

$$\phi_k = a\tan[\mathrm{imag}(m_k)/\mathrm{real}(m_k)]. \tag{7}$$

This is the general theory behind this method, which is written here for a single pair of sensors. A more detailed description, including orientation estimation for several pairs of sensors based on simultaneous use of multiple teleseismic events, as well as uncertainty estimation, can be found in Grigoli *et al.* (2012). We omit details here for the sake of brevity.

In the case of RSC, our goal is to calculate the relative misalignment angles between each borehole station and ED06. As a mandatory requirement, the distance between the stations must be much smaller than the dominant wavelength of the signal used, that is,

$$d \ll \lambda. \tag{8}$$

Ⓔ Table S1 shows the approximate distances of the RSC stations to the reference station ED06. The distances range from a couple of kilometers to a maximum of about 10 km.

Taking into account condition (8), we selected the seismograms used for the determination of the rotation angles on the basis of the following conditions:

- teleseismic events with epicentral distances of at least 5000 km from RSC;
- a lower magnitude limit of 6.0 (M_w) and enough energy to be recorded simultaneously by all RSC stations in the frequency band of interest (see next point); and
- frequency band of 0.08–0.15 Hz, which ensures a minimum wavelength much larger than 10 km. Although at the low-end limit, this frequency band is fine for Güralp SP1 seismometers.

Obviously the search interval was limited to that of the RSC life, that is, from 1 January 2012 to 31 May 2014, when this study ended.

The Incorporated Research Institutions for Seismology (IRIS) database was searched for earthquake data using the Wilber 3 (web-based event explorer) tool (see Data and Resources). Seismograms were extracted and downloaded in Seismic Analysis Code (SAC) format (Goldstein *et al.*, 2003; Helffrich *et al.*, 2013) from the National Institute of Oceanography and Experimental Geophysics (OGS) Archive System of Instrumental Seismology (OASIS) database (Priolo, Laurenzano, *et al.*, 2015).

RESULTS AND DISCUSSION

To test the whole procedure, we start with a very energetic teleseismic event that occurred in the Pacific Ocean near the Solomon Islands and with the following characteristics: date and time (UTC), 19 April 2014 13:28:00; location, Solomon Islands; latitude, −6.75°; longitude, 155.024°; magnitude, 7.5 M_{WW} (US); and depth, 43.4 km.

For all stations, the signal was preprocessed in the following way: (1) it is downsampled by decimation from 200 to 1 Hz sampling; (2) static offset and linear trend are removed, and 5% tapering is applied; and (3) the signal is filtered in the 0.08–0.15 Hz frequency band using a Butterworth fourth-order band-pass filter. Figure 3 shows an example of the Solomon Island earthquake signal recorded by ED06, ED09, and ED10 stations and preprocessed according to the procedure described above.

The calculations were performed using MATLAB scripts. The original programs of Grigoli *et al.* (2012) have been slightly modified to take into account the phase delay between the recorded waveforms at two different stations by including the time-shift estimation directly within the inversion process. The results obtained at the end of the test phase are shown in Table 1. The table is divided into two parts: the left side shows the angles estimated for each station using station ED06 as a reference, and the right side reports a sample of the angles estimated by cross referencing each station to the other stations. In the latter case, only a subset of the results is presented, that is, we include only the station pairs ED($i + 1$) versus ED(i), in which ED(i) is taken as a reference station, and $i = 1, ..., 10$.

The values obtained using station ED06 as a reference show that the misalignment usually ranges within a 10° range, but, for stations ED07 and ED09, quite large misalignment angles are observed. For station ED09, we have already men-

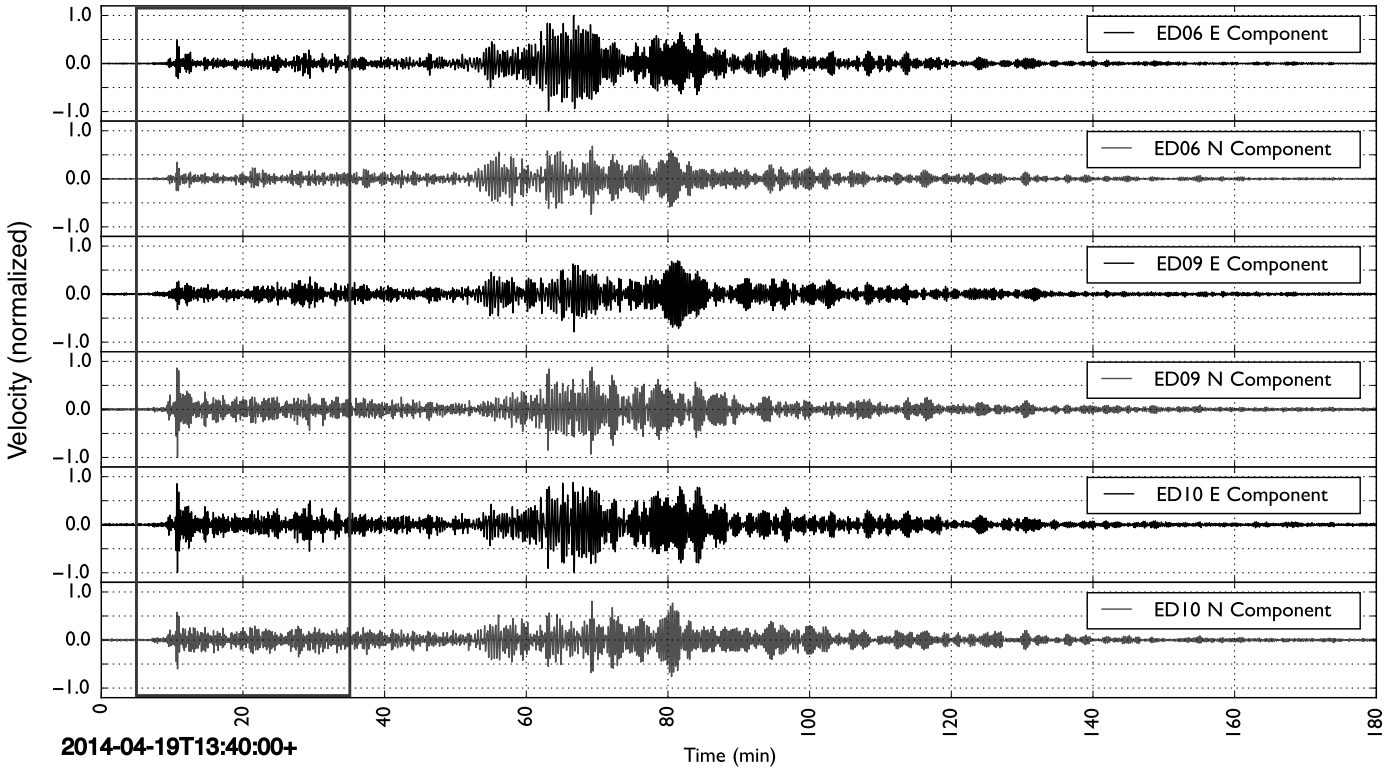

▲ **Figure 3.** Example of traces used for the horizontal alignment calculation. Seismograms refer to the Solomon Islands M_w 7.5 earthquake recorded by ED06, ED09, and ED10 stations. The two horizontal components (labeled as east [E] and north [N]) are shown. The gray box to the left side indicates the partition of the waveform shown in Figure 4, and the hodograms shown in Figure 5.

tioned that its sensor was not aligned. For the other stations, misalignment angle is often smaller than 5°, and this demonstrates that the simple method used to deploy and orientate the borehole sensor was quite effective. Surprisingly, also the value of 7.74° obtained for station ED01 is quite good, if we consider that the sensor lies at 150 m depth.

To evaluate the robustness of the method against the choice of the reference station, we have computed the misalignment by cross referencing each station to all the other stations. The right column of Table 1 shows a sample representative of such measurements. It can be clearly seen that the values obtained by cross referencing two arbitrary stations correspond nearly exactly to the algebraic sum of those obtained for the same stations using station ED06 as a reference.

We apply the orientation method to the whole seismic trace. However, for display purposes, we show only a limited part of seismograms, which corresponds to the box drawn in Figure 3. Furthermore, we show examples (following Figs. 4 and 5) only

Table 1
Misalignment Angles Obtained for the Test Event (M_w 7.5 of the 19 April 2014, 13:28:00 UTC at Solomon Islands)

Reference Station ED06		All Stations to All Stations	
Pair of Stations	**Angles (°)**	**Pair of Stations**	**Angles (°)**
ED06 vs. ED01	−7.74 ± 0.12	ED02 vs. ED01	−4.02 ± 0.20
ED06 vs. ED02	−2.84 ± 0.12	ED03 vs. ED02	0.97 ± 0.11
ED06 vs. ED03	−3.30 ± 0.12	ED04 vs. ED03	9.48 ± 0.10
ED06 vs. ED04	5.44 ± 0.10	ED05 vs. ED04	8.34 ± 0.09
ED06 vs. ED05	−3.65 ± 0.10	ED06 vs. ED05	−3.65 ± 0.10
ED06 vs. ED07	*−14.72 ± 0.09*	ED07 vs. ED06	14.72 ± 0.09
ED06 vs. ED08	−0.01 ± 0.08	ED08 vs. ED07	−14.46 ± 0.07
ED06 vs. ED09	*−38.14 ± 0.10*	ED09 vs. ED08	38.66 ± 0.07
ED06 vs. ED10	0.61 ± 0.13	ED10 vs. ED09	−42.92 ± 0.08

Uncertainty corresponds to the first standard deviation. Italicized values denote the largest misorientation angles.

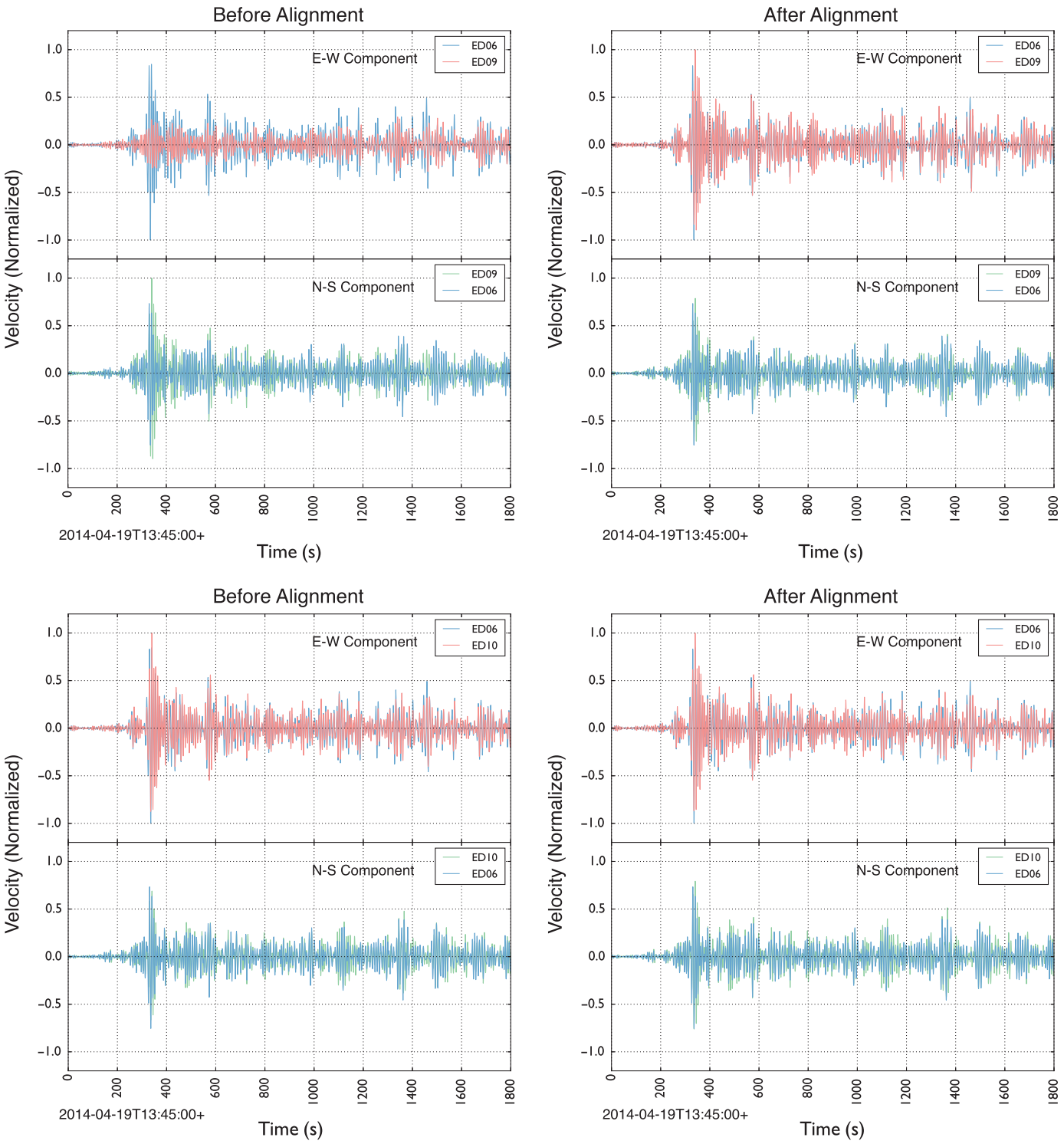

▲ **Figure 4.** Comparison of the seismograms (left) before and (right) after misalignment correction. Station pairs ED06–ED09 and ED06–ED10 are shown in the upper and lower panels, respectively. Each panel shows both horizontal components (i.e., east–west [E-W] and north–south [N-S]), for an 1800-s-long time window, which is used only for display purposes. Seismograms are band-pass filtered in the 0.08–0.15 Hz window. The blue traces always correspond to the reference station ED06, whereas the green and red colors correspond to the north–south and east–west components of the other stations.

for the two sensor couples ED06–ED09 and ED06–ED10, which represent the worst and best orientation conditions, respectively. Figures 4 and 5 show the seismograms and hodograms, respectively, before and after alignment. As seen in Table 1, these two stations feature very different misalignment values, that is, a very large angle of about 38° for ED09 and a quite small angle of

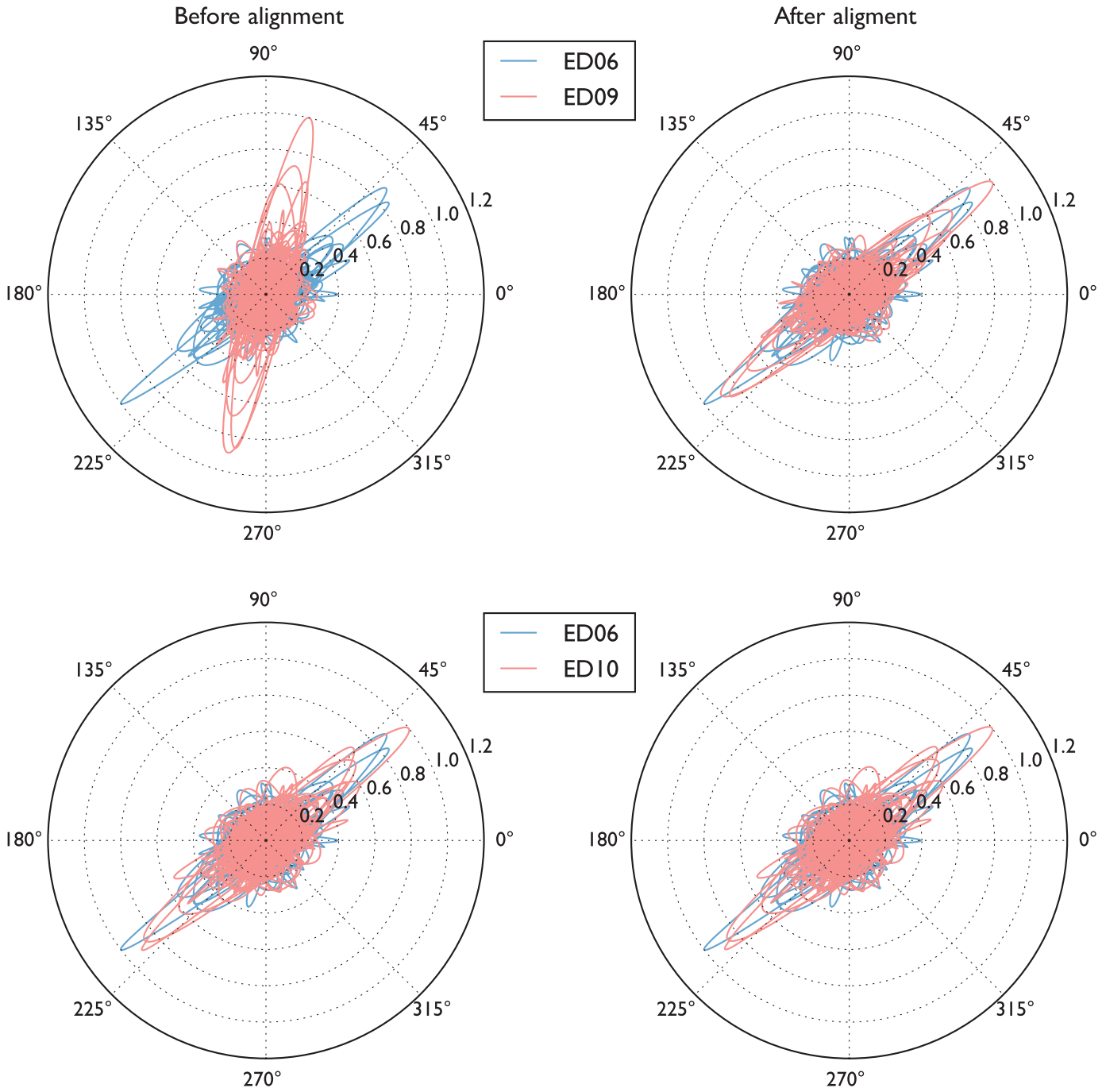

▲ **Figure 5.** Particle motion (hodograms) related to station pairs (left), as shown before and (right) after misalignment correction. Panels along horizontal levels show the misalignment correction for the worst and best cases, respectively, described in Ⓔ Table S2, that is, (top) ED06 versus ED09 with rotation angle of −38.14° and (bottom) ED06 versus ED10 with rotation angle of −0.61°. ED06 is represented in blue, whereas ED09 and ED10 are represented in red.

less than 1° for ED10. In both cases, the adopted procedure turns out to be very effective, despite the initial differences among the signals. In both cases, it can also be appreciated how the estimated misalignment angle corresponds to the angle that minimizes the misfit between complex traces.

Having verified the procedure for one earthquake, we can apply it to align all the RSC sensors for the whole period considered in this study. For each continuous operational period of each sensor, we have selected one or more teleseismic events according to the criteria defined above. Table 2 lists the whole group of earthquakes. Earthquake 7 corresponds to that used for the calibration procedure described previously. Note that we have used more events simultaneously, when available, in a single inversion step by appending traces of different events

Table 2
Earthquakes Used for the Estimation of the Alignment Angles of the Period 1 January 2012 to 31 May 2014

ID Number	Earthquake	Date (yyyy/mm/dd)	Time (UTC) (hh:mm:ss)	Latitude	Longitude	Depth (km)	M_w
1	West Coast Sumatra	2012/01/10	18:37:00	2.433° N	93.21° E	20.9	7.2
2	Solomon Islands	2012/07/25	11:20:27	9.694° S	159.61° E	20	6.4
3	Sea of Okhotsk	2012/08/14	02:59:38	49.8° N	145.06° E	583.2	7.7
4	Vanuatu Islands	2012/12/21	22:28:08	14.34° S	167.29° E	200.7	6.7
5	Santa Cruz Islands	2013/02/06	01:23:19	11.25° S	164.93° E	10.1	7.1
6	Coast of Peru	2013/09/25	16:42:43	15.83° S	74.51° W	40	7.1
7	Guerrero, Mexico	2014/04/18	14:27:24	17.397° N	100.97° W	24	7.2
8	Solomon Islands	2014/04/19	13:28:00	6.75° S	155.02° E	43.4	7.5

sequentially to form a single trace. Uncertainties are estimated as described by Grigoli *et al.* (2012).

The obtained results are summarized in Ⓔ Table S2. First of all, it can be seen that many sensors were removed and redeployed, changed several times due to malfunctions. Basically the stations mostly affected by changes were ED01, ED05, ED06, ED08, and ED09, whereas the other stations show a more stable behavior. Most misalignment angles range within about ±5°, whereas the largest values are of some tens of degrees, as for instance for station ED09. Although the technique adopted for aligning the borehole sensors by acting from the ground surface proves to be quite effective in several cases (e.g., ED02, ED03, ED08, ED10, and even ED01, at about 150 m depth), we remark that, in the absence of direct control of the orientation, the misalignment estimation is absolutely needed to ensure a correct use of the recorded data.

To further validate our results, we apply the same procedure to those stations that are equipped with an accelerometer at the surface, using the accelerometer as a reference. Because accelerometers are much less sensitive than seismometers, we focused only on the most energetic signals recorded by the network for the teleseismic events of Table 2, that is, those of the M_w 7.5 Solomon Islands earthquake. To improve the waveform similarity between the two sensors, we corrected the signal recorded by the broadband sensors for their instrument response and calculated the derivative of the velocity waveforms to obtain accelerograms. We then filtered all accelerograms in the 0.08–0.15 Hz frequency range. In all cases, we observed misalignment angles of a few degrees; misalignment was always less than 5° and therefore was within the reasonable margin of errors that we expect for manual compass-based orientation. Ⓔ As an example, the electronic supplement reports the results obtained for site ED05, for which the borehole seismometer features an orientation misalignment of about 1.5° with respect to the surface accelerometer. (Recall that the misalignment estimated with respect to station ED06 was 3.65°; Table 2.) This test further demonstrates the reliability of our results.

CONCLUSIONS

In this article, we estimated the borehole sensor orientation of the RSC using the technique developed by Grigoli *et al.* (2012), based on the estimation of relative orientation angles among different station pairs by fitting the complex traces of each station pair using a complex linear least-squares approach. In this study, we used seven different teleseismic events within the magnitude (M_w) range of 6.4–7.7. This method can be applied when the distance between the misoriented stations and the reference station is smaller than the dominant wavelength of the signal used. Because the interstation distances of the RSC range from a couple of kilometers to a maximum of about 10 km, seismograms were analyzed in the 0.08–0.15 Hz frequency band. We always estimated the orientation angle using a well-oriented reference station (i.e., ED06 for RSC) for which the orientation can be controlled manually. However, we also found that the relative angle between two generic sensors corresponds with the algebraic sum of the misalignments estimated independently with respect to a reference sensor using different earthquakes. Thus, this technique may easily adapt to different situations.

After a first phase of check and calibration on the network features, the adopted method performed well and has been shown to be very effective, and it can easily be used to estimate the horizontal orientation after each operationial change on the sensor. We found that misalignment angles range from a few degrees to some tens of degrees, and they are not necessarily correlated to the sensor depth. As a matter of fact, there can be several reasons why the sensor is not aligned, despite all precautions. The fact is that, in the absence of direct control on the orientation, the verification of the horizontal alignment is mandatory for whomever manages a network, if the goal is to deliver a high-quality standard.

DATA AND RESOURCES

Information and data on the Collalto Seismic Network (RSC) can be found at http://rete-collalto.crs.inogs.it (last accessed June 2015). The full dataset of continuous waveforms of the RSC is freely available at the National Institute of Oceanography and Experimental Geophysics (OGS) Archive System of Instrumental Seismology (OASIS; http://oasis.crs.inogs.it/, last accessed June 2015), which is the database that archives the instrumental seismological data of the OGS. The Incorporated Research Institutions for Seismology (IRIS) consortium is

available at http://ds.iris.edu (last accessed June 2015). IRIS Wilber 3 is the database of world earthquakes and web-based event explorer (http://ds.iris.edu/wilber3/find_event, last accessed June 2015).

ACKNOWLEDGMENTS

The Collalto Seismic Network (RSC) was developed and is managed by the National Institute of Oceanography and Experimental Geophysics (OGS) on behalf of Edison Stoccaggio S.p.A. (i.e., Italian Società per Azioni) under the requirements of the Italian Ministry for the Environment and Land and Sea Protection and in agreement with the Veneto Region. This study was partially funded by the International Centre of Theoretical Physics (www.ictp.org, last accessed June 2015) under the Training and Research Program in Italian Laboratory (TRIL) Programme (https://www.ictp.it/tril.aspx), with a grant awarded to Eduardo Diez Zaldívar; the Italian Ministry for the Economic Development (MiSE), General Directorate for the Mining Resources (DGRME, http://unmig.sviluppoeconomico.gov.it/), within the Program Agreement with OGS (Record Number 3835 of the Corte dei Conti) under Activity 1, entitled "Development of analysis methods for a rapid correlation of the detected seismicity to the underground exploitation for energy production"; and the German Ministry of Education and Research (BMBF), under project MINE (Grant Number BMBF03G0737A), which is part of the research and development program GEOTECHNOLOGIEN. Finally, we thank our colleagues of the OGS, CRS Section, Marco Romanelli, Milton Plasencia Linares, and Adelaide Romano, as well as Edison Stoccaggio S. p. A. for their help in several phases of this work.

REFERENCES

Becquey, M., and M. Dubesset (1990). Three-component sonde orientation in a deviated well, *Geophysics* **55,** no. 10, 1386–1388.

Di Siena, J. P., J. E. Gaiser, and D. Corrigan (1984). Horizontal components and shear wave analysis of three components VSP data, in *Vertical Seismic Profiling, Part B: Advance Concepts*, M. N. Toksöz and R. R. Steward (Editors), Geophysical Press, London, United Kingdom, 175–235.

Goldstein, P., D. Dodge, M. Firpo, and Lee Minner (2003). SAC2000: Signal processing and analysis tools for seismologists and engineers, in *The IASPEI International Handbook of Earthquake and Engineering Seismology*, W. H. K. Lee, H. Kanamori, P. C. Jennings, and C. Kisslinger (Editors), Academic Press, London.

Grigoli, F., S. Cesca, T. Dahm, and L. Krieger (2012). A complex linear least-squares method to derive relative and absolute orientations of seismic sensor, *Geophys. J. Int.* **188,** no. 3, 1243–1254, doi: 10.1111/j.1365-246X.2011.05316.x.

Gruppo di Lavoro MPS (2004). Redazione della mappa di pericolosità sismica prevista dall'Ordinanza PCM 3274 del 30 marzo 2003, *Rapporto conclusivo per il Dipartimento di Protezione Civile*, Istituto Nazionale di Geofisica e Vulcanologia (INGV), Milano–Roma, April 2004, 65 pp.+ 5 appendixes (in Italian), http://zonesismiche.mi.ingv.it/documenti/rapporto_conclusivo.pdf (last accessed January 2015).

Helffrich, G., J. Wookey, and I. Bastow (2013). *Seismic Analysis Code (SAC), a Primer and User's Guide*, Cambridge University Press, Cambridge, United Kingdom, ISBN: 9781107613195.

Hensch, M. (2009). On the interrelation of fluid-induced seismicity and crustal deformation at the Columbo submarine volcano (Aegean Sea, Greece), *Ph.D. Thesis*, University of Hamburg, Hamburg, Germany.

Krieger, L., and F. Grigoli (2015). Optimal reorientation of geophysical sensors: A quaternion-based analytical solution, *Geophysics* **80,** no. 2, F19–F30, doi: 10.1190/geo2014-0095.1.

Michaels, P. (2001). Use of principal component analysis to determine down-hole tool orientation and enhance SH-waves, *J. Environ. Eng. Geophys.* **6,** no. 4, 175–183.

Nakamura, Y., P. I. Donoho, P. H. Roper, and P. M. McPherson (1987). Large off-set seismic surveying using ocean-bottom seismographs and air gun: Instrumentation and field technique, *Geophysics* **52,** no. 12, 1601–1612.

Oye, V., and W. I. Ellsworth (2005). Orientation of three-component geophones in the San Andreas Fault Observatory at Depth pilot hole, Parkfield, California, *Bull. Seismol. Soc. Am.* **95,** no. 2, 751–758.

Picotti, V. (2007). Relazione geologica di inquadramento del giacimento "Conegliano" e analisi dei possibili rischi geologici dovuti all'attivitàdi "Collalto Stoccaggio," Edison Stoccaggio S.p.A., *Internal Rept.*, 18 pp. (in Italian).

Priolo, E., G. Laurenzano, C. Barnaba, B. Bernardi, L. Moratto, and A. Spinelli (2015). OASIS: The OGS archive system of instrumental seismology, *Seismol. Res. Lett.* **86,** no. 3, 978–984 + esupp, doi: 10.1785/0220140175.

Priolo, E., M. Romanelli, M. P. Plasencia Linares, M. Garbin, L. Peruzza, M. A. Romano, P. Marotta, P. Bernardi, L. Moratto, D. Zuliani, and P. Fabris (2015). Seismic monitoring of an underground natural gas storage facility: The Collalto Seismic Network, *Seismol. Res. Lett.* **86,** no. 1, 109–123 and electronic supplement, doi: 10.1785/0220140087.

Zha, Y., and W. Menke (2013). Determining the orientations of ocean bottom seismometers using ambient noise correlation, *Geophys. Res. Lett.* **40,** 1–6, doi: 10.1002/grl.50698.

Zheng, X. Y., and G. A. McMechan (2006). Two methods for determining geophone orientation from VSP data, *Geophysics* **71,** no. 4, V87–V97.

Eduardo R. Diez Zaldívar
Centro Nacional de Investigaciones Sismológicas (CENAIS)
C.P. 90400
Santiago de Cuba, Cuba
diez@cenais.cu

Enrico Priolo
Francesco Grigoli
Istituto Nazionale di Oceanografia e di Geofisica Sperimentale (OGS)
Sezione Scientifica Centro di Ricerche Sismologiche (CRS)
Borgo Grotta Gigante 42/C
34010 Sgonico
Trieste, Italy
epriolo@inogs.it
fgrigoli@inogs.it

Simone Cesca
German Research Centre for Geosciences (GFZ)
Telegrafenberg, 14473
Potsdam, Germany
simone.cesca@gfz-potsdam.de

Published Online 23 March 2016